Cryogenic linear ion trap for accurate spectroscopy

M. E. Poitzsch,[a] J. C. Bergquist, W. M. Itano, and D. J. Wineland
Time and Frequency Division, National Institute of Standards and Technology, Boulder, Colorado 80303

(Received 15 May 1995; accepted for publication 11 October 1995)

We have observed linear ''crystals'' of up to tens of laser-cooled $^{199}Hg^+$ ions in a linear rf ion trap. The trap operates at liquid-He temperature and is designed for use as a prototype 40.5 GHz frequency standard with high accuracy and stability. © *1996 American Institute of Physics.* [S0034-6748(96)05001-1]

I. INTRODUCTION

The 40.5 GHz ground-state hyperfine transition of the $^{199}Hg^+$ ion provides the basis for a high-performance microwave frequency standard.[1–5] Our work on $^{199}Hg^+$ has been devoted to obtaining a system that will provide high accuracy as well as high stability.[5] To help achieve this goal, we have incorporated laser cooling to suppress the second-order Doppler shift.

In this paper, we report preliminary results using a rf ion trap in a cryogenic (~4 K) environment. This should yield high vacuum, thereby reduce ion loss and frequency shifts due to background gas collisions, should provide the basis for superconducting magnetic shielding, and will suppress shifts due to blackbody radiation.[6]

Figure 1 shows the energy levels of interest in the $^{199}Hg^+$ ion. The $^2S_{1/2}(F=1,M=0)$ to $^2S_{1/2}(F=0,M=0)$ ground-state hyperfine splitting is ~40.5 GHz. It has no first-order Zeeman shift near zero field and is used as the clock transition.[1–5] The upper-state $^2P_{1/2}(F=1)$ to $^2P_{1/2}(F=0)$ hyperfine splitting is ~7 GHz. Laser cooling and fluorescence detection are accomplished using the 194 nm electric dipole cycling transition from the ground $^2S_{1/2}(F=1)$ state to the excited $^2P_{1/2}(F=0)$ state.[5,7] The natural linewidth of this strongly allowed transition is 70 MHz, which is more than an order of magnitude larger than the width of the 194 nm laser used for cooling and detection. To prevent optical pumping of the ion into the $F=0$ ground-state sublevel by off-resonant driving of the $^2S_{1/2}(F=1)$ to $^2P_{1/2}(F=1)$ transition and subsequent decay, a second (collinear) laser at 194 nm is present during the laser cooling and tuned about 47.4 GHz to the blue of the main cooling laser.

Previously, a rf-trap $^{199}Hg^+$ ion frequency standard (using helium buffer gas cooling) was shown to have high frequency stability.[3] It contained $N\approx 2\times 10^6$ ions and had a fractional second-order Doppler shift of approximately -2×10^{-12}. More recently, a short-term fractional frequency instability of $<7\times 10^{-14}\,\tau^{-1/2}$ has been demonstrated in a linear rf trap (also using helium buffer gas cooling), which operated with $N\approx 2.5\times 10^6$ ions, and a fractional second-order Doppler shift of approximately -4×10^{-13} was inferred.[4] In comparison, the fractional second-order Doppler shift of a single $^{199}Hg^+$ ion laser cooled to the Doppler limit is about -2×10^{-18} (see Ref. 8). The fractional frequency shift of the 40.5 GHz clock transition with magnetic field is $0.24B^2$, where B is expressed in teslas. Thus, a $^{199}Hg^+$ ion confined in an ion trap at near-zero magnetic field and laser cooled to the Doppler limit should constitute a highly accurate 40.5 GHz microwave frequency standard. To improve the signal-to-noise ratio (and hence the fractional frequency stability), it will, however, be desirable to have many $^{199}Hg^+$ ions, all with equally low Doppler shifts.

II. LINEAR RF ION TRAP

The linear rf quadrupole trap, which uses four rf rods for radial confinement and a static axial potential for longitudinal confinement, was developed as a way of confining multiple ions with low Doppler shifts due to rf micromotion.[4,5,9–11] In this scheme, the four rods are configured as in a rf mass analyzer, with a zero-field node along the center line instead of at a single point as in a spherical Paul quadrupole rf trap.[12] Axial confinement is achieved by applying static potentials at the ends of the trap, using positively biased rings, pins, or split sections in the trap rods. Figure 2 shows the linear rf trap used in the present cryogenic experiment. The four rf rods are $R'=0.20$ mm in radius, centered on a radius of $R+R'=0.64$ mm from the trap axis (about half the size of our previous linear rf trap[5]). Axial confinement is achieved by positively biasing rings (electrodes C and R in Fig. 2), separated by 4 mm, at either end of the four-rod quadrupole.

Two (diagonally opposite) rf rods of the trap are driven with a rf potential $V_0\cos(\Omega t)$, while the other two rf rods are maintained at rf ground. Near the trap axis, the time-varying potential is approximately a saddle-point potential in x and y,

$$V(x,y)\approx \frac{V_0}{2}\left(1+\frac{x^2-y^2}{R^2}\right)\cos(\Omega t), \tag{1}$$

where x and y are the transverse coordinates. The centers of the two rf-driven rods intersect the x axis, one at $-(R+R')$ and the other at $R+R'$. The approximation assumes that the rods of circular cross section give the same potential as rods whose surfaces are equipotentials of Eq. (1). If the drive frequency Ω is high enough (that is, much higher than the ion's radial secular oscillation frequency), the ion of mass m and charge q will experience an approximately harmonic pseudopotential that confines in both x and y:

[a]Present address: Schlumberger-Anadrill, Sugar Land, TX 77778.

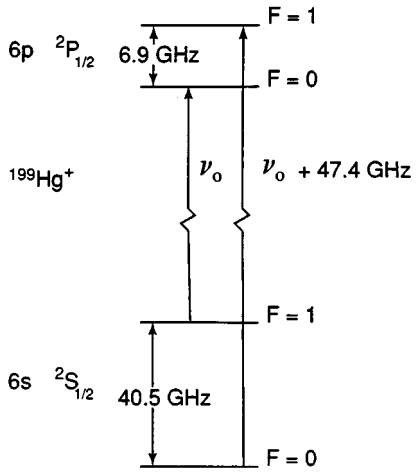

FIG. 1. Diagram of the hyperfine energy levels of the $^{199}Hg^+$ ground $6s^2S_{1/2}$ state and the $6p^2P_{1/2}$ state. Here ν_0 corresponds to a wavelength of 194.2 nm. The 40.5 GHz ground-state hyperfine transition is intended for use as a reference for a frequency standard.

$$\Phi(x,y) \approx \frac{m}{2q}\,\omega_r^2(x^2+y^2), \tag{2}$$

where ω_r is the radial angular oscillation frequency (secular frequency), which is given by

$$\omega_r = \frac{qV_0}{\sqrt{2}m\Omega R^2}. \tag{3}$$

Axial confinement (along z) results from biasing the rings at either end of the trap with a positive potential U_0. Near the center of the trap, an ion experiences the static saddle-point potential

$$\phi_s(x,y,z) \approx \frac{m}{2q}\,\omega_z^2[z^2 - \tfrac{1}{2}(x^2+y^2)], \tag{4}$$

where the axial angular oscillation frequency ω_z is given by

$$\omega_z = \left(\frac{2\kappa q U_0}{mz_0^2}\right)^{1/2}. \tag{5}$$

The separation of the rings is $2z_0 = 4.0$ mm, and κ is a geometrical factor that is ~ 0.004 in this trap (as determined from measurements of ω_z). As Eq. (4) indicates, the radial pseudopotential Φ is weakened by the addition of the static axial potential. Thus, the effective radial angular oscillation frequency is

$$\omega_r' = (\omega_r^2 - \omega_z^2/2)^{1/2}. \tag{6}$$

Under typical operating conditions in this trap, we expect $\omega_r'/2\pi \approx 350$ kHz and $\omega_z/2\pi \approx 25$ kHz, assuming $\Omega/2\pi = 13$ MHz, $V_0 = 100$ V, and $U_0 = 25$ V.

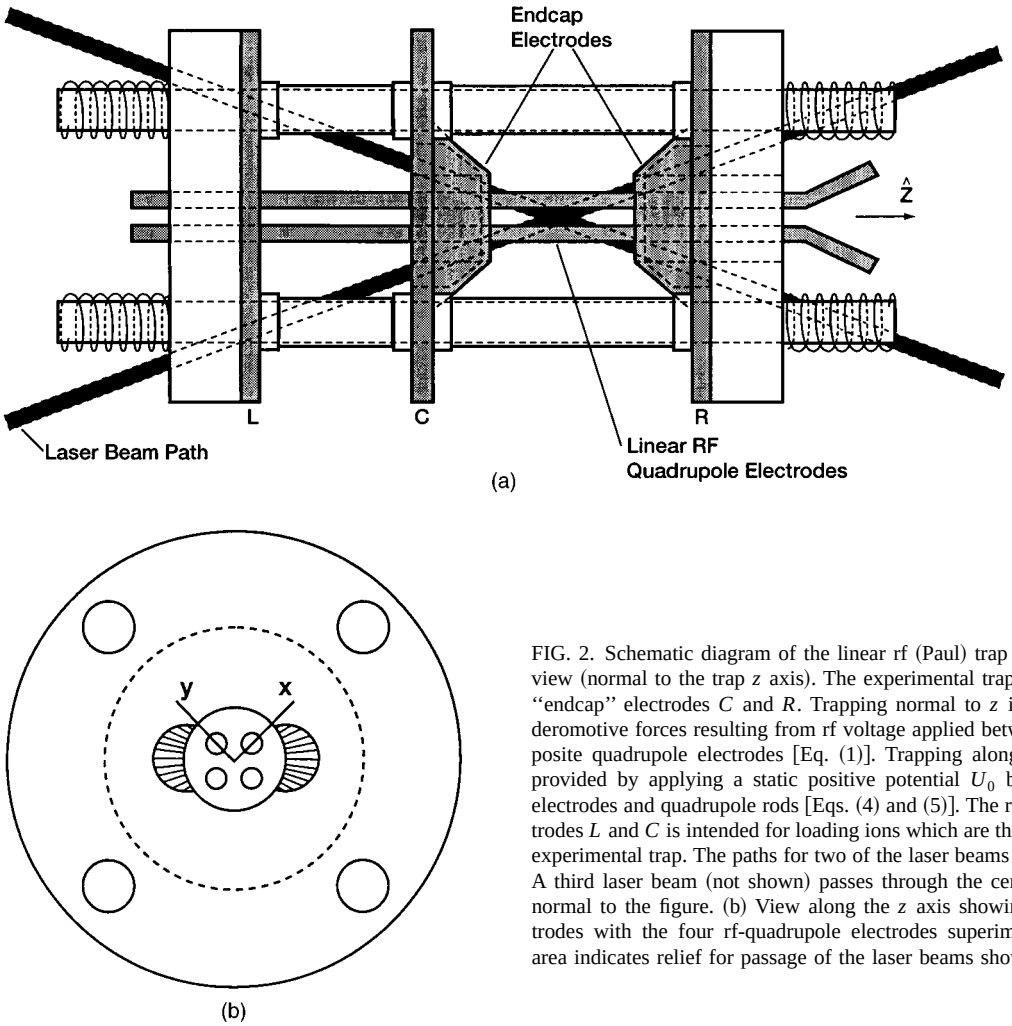

FIG. 2. Schematic diagram of the linear rf (Paul) trap electrodes. (a) Side view (normal to the trap z axis). The experimental trap is located between "endcap" electrodes C and R. Trapping normal to z is provided by ponderomotive forces resulting from rf voltage applied between diagonally opposite quadrupole electrodes [Eq. (1)]. Trapping along the z direction is provided by applying a static positive potential U_0 between the endcap electrodes and quadrupole rods [Eqs. (4) and (5)]. The region between electrodes L and C is intended for loading ions which are then transferred to the experimental trap. The paths for two of the laser beams are shown in black. A third laser beam (not shown) passes through the center of the trap and normal to the figure. (b) View along the z axis showing the endcap electrodes with the four rf-quadrupole electrodes superimposed. The shaded area indicates relief for passage of the laser beams shown in (a).

As shown in Fig. 2, the trap's axial-confinement ''ring'' electrodes are in fact, bored-out conical disks of beryllium copper, appropriately drilled to allow laser access to the trap center. The four rf rods are beryllium-copper wires. The dimensions of the quadrupole rods were chosen to allow $f/1$ light collection from the center of the trap. Also, the choice of the small R dimension makes the trap radially unstable, due to the Mathieu instability, for unwanted contaminant ions (created during the loading procedure) with $\omega_r > \Omega/2$ or, equivalently

$$m \leqslant 10.6u \times \left(\frac{V_0}{100\ \mathrm{V}} \right), \tag{7}$$

where u is the atomic mass unit. The four outer support rods for the trap structure are alumina (Al_2O_3) rods sheathed in thin beryllium-copper tubing of an outer diameter of 1.28 mm. These support rods can each receive independent biasing potentials to ''shim'' the ions back onto the trap's geometrical center line, in the event that patch charges on the rod electrodes should cause the trap's geometrical and dc electrical centers to not coincide. (Without this compensation, the ions could experience large rf electric fields and undergo substantial rf micromotion.) The ceramic insulating endpieces that define the positions of the trap rods are high-purity alumina slabs 2.0 mm in thickness, with appropriately placed laser beam access holes.

Figure 2(a) shows that the electrodes form two linear traps in tandem. The leftmost trap, between electrodes L and C, is intended for capturing ions in the initial loading process. Ions would then be pushed through electrode C into the experimental trap (between electrodes C and R). This design was implemented with the idea of gaining immunity from contact potentials or electric charge buildup on the electrodes near where the ions were loaded.

Appropriately placed mirrors allow laser cooling to be performed along any one of three noncoplanar directions at the center of the trap, as illustrated in Fig. 2(a): in the plane of the page at $\pm 20°$ to the trap's z axis or normal to the plane of the page (using a small mirror located directly below the trap). We require only one of the beams shown in Fig. 2(a) for cooling, optical pumping, and detection. The three beam paths are required for probing the velocity distribution in three dimensions. The kinetic temperatures achievable in these cooling geometries are derived using Ref. 13. The temperatures at the Doppler-cooling limit with either of the $\pm 20°$ beams correspond to $T_{\mathrm{radial}} \approx 5.6$ mK and $T_{\mathrm{axial}} \approx 1.2$ mK, under the assumption that the radiation is emitted isotropically. These temperatures imply a fractional second-order Doppler shift of the 40.5 GHz hyperfine transition frequency that is approximately -5.5×10^{-18}.

Previously, a slightly larger linear rf trap, in which the rods were segmented in such a way that dc potential differences could be applied to the different segments, was used, thus providing axial confinement.[5] In that apparatus, operating at room temperature and at a pressure of about 10^{-8} Pa, several tens of $^{199}Hg^+$ ions were crystallized at fixed positions in a single row along the trap's nodal center line. Such a geometry is optimal for the present frequency standard application, since the ions can be imaged independently for improved signal-to-noise ratio, and all have approximately the same low second-order Doppler shift as a single ion in a quadrupole trap. The major limitation of this previous apparatus was the background gas pressure in the vacuum chamber, which was high enough that ions would be lost in several minutes due to chemical reactions. For a frequency standard application, it is desirable to be able to interrogate a particular ensemble of ions, located at relatively fixed positions, for periods of many hours, several days, or longer. Also, even at 10^{-8} Pa, shifts of the transition frequency with changes in the background gas pressure could limit the accuracy.[14]

III. CRYOGENIC LINEAR RF ION TRAP

Our solution to the background gas pressure problem is to maintain the trap and vacuum vessel at liquid-He temperature ($\sim$4 K). At this low temperature, most gases cryopump to the walls of the chamber, giving a very low background pressure. In a similar sealed vacuum can, lowered to 4 K, Gabrielse *et al.*[15] report background pressures below 10^{-14} Pa. Thus by lowering the pressure by several orders of magnitude, we should be able to store trapped ions for at least several days, interrogate them with Ramsey free-precession times as long as tens or hundreds of seconds, and eliminate or greatly reduce pressure shifts of the 40.5 GHz clock frequency. In addition, the 4 K temperature should allow us to operate a superconducting shield around the ion trap region to help in shielding changes in the magnetic field.

We have constructed and have made initial tests of a prototype apparatus based on these concepts. The trap described in Sec. II and related components are mounted in an In-sealed OFHC copper vacuum can (see Fig. 3), inside a nested liquid-He/liquid-N_2 Dewar, heat sunk to the outside bottom of the liquid-He reservoir and surrounded by radiation shields at 4 and 77 K. Figure 4 shows a schematic view of the small vacuum can mounted inside its nested liquid-He/liquid-N_2 Dewar, which has a liquid-He hold time of about four days. Optical access to the trap region is through windows around the base of the Dewar, aligned with baffled holes in the radiation shields and windows in the sides of the can. The laser beams are introduced into the vacuum apparatus through In-sealed fused silica windows.[16] Electrical and microwave access is through heat-sunk cabling leading down from connectors on the Dewar's top vacuum flange. The cables are routed along the liquid-N_2 and liquid-He reservoirs, into the radiation-shielded 4 K space around the experimental vacuum can, to cryogenic vacuum feedthroughs on the sides of the can. The 13 MHz rf drive for the trap (see below) and the dc currents for the field coils surrounding the trap are routed down the neck of the Dewar, through the liquid-He, and into the can by cryogenic feedthroughs in its top plate (which is also the bottom plate for the liquid-He reservoir). The superconducting shield consists of a 5 μm coating of lead, electroplated onto the inside of the copper vacuum vessel.

The rf potential V_0 is applied to the trap electrodes by a resonant step-up transformer. In the frequency range of interest here, the most convenient type of resonator consists of a helical ''secondary'' coil that is effectively $\lambda/4$ in length in-

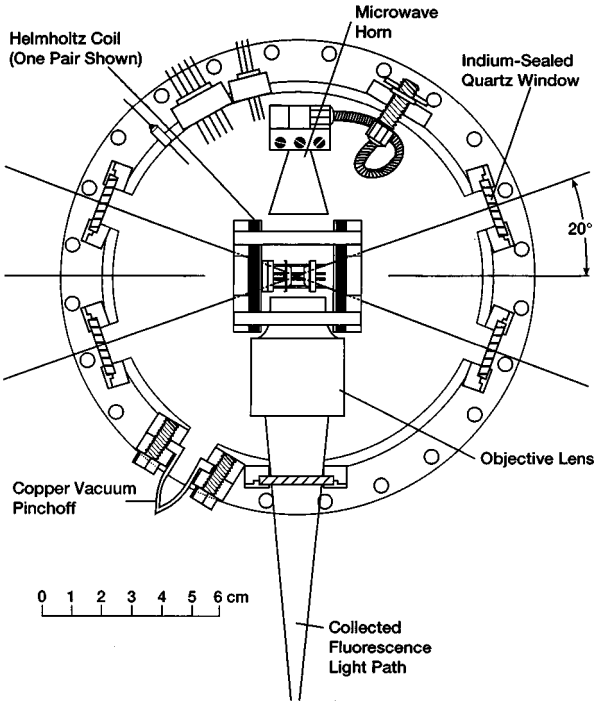

FIG. 3. Top view of pillbox vacuum assembly. The trap is shown at the center of the diagram in the same orientation as Fig. 2(a). Two of the laser beam paths are shown at 20° with respect to the trap z axis. The top of this pillbox asssembly forms the bottom of the liquid-He reservoir shown in Fig. 4.

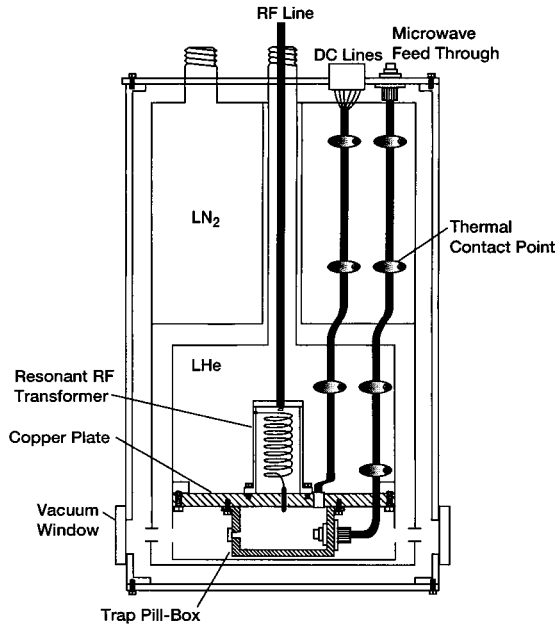

FIG. 4. Side view of cryostat assembly (not to scale). The pillbox containing the trap and related hardware is bolted to a copper plate which forms the bottom of the liquid-He reservoir. The resonant rf transformer is shown on top of this copper plate. The high-voltage output lead is connected to a vacuum feedthrough which is then connected to the trap quadrupole electrodes inside the trap pillbox.

side a shielding cylindrical can,[17] with an inductive-coupling input ''primary'' loop at the end of the input coaxial line. In our cryogenic apparatus, it is desirable to dissipate as little rf power as possible into the liquid helium. Thus, we constructed a superconducting lead helical resonator with $Q \approx 3000$ when attached to the trap apparatus. The losses are mainly in the connecting leads and not in the resonator. (The resonator by itself had an unloaded Q in excess of 200 000.) It was determined that 4 mW of rf at 13 MHz produced an amplitude $V_0 \approx 150$ V at the trap rods. The superconducting resonator sits at the bottom of the Dewar reservoir, immersed in liquid He, with the high-potential end of its secondary coil attached to a copper cryogenic feedthrough leading through the top plate of the experimental vacuum chamber and connected to the two rf-driven rods of the trap. The input coupling loop is a small off-axis coil, attached to a stainless-steel coaxial cable leading out through the top of the Dewar through an O-ring compression seal. This coaxial cable can be rotated from outside the Dewar so as to orient the coupling loop properly for optimized power coupling into the resonator.

The trap is surrounded by orthogonal pairs of small coils, each consisting of 350–600 turns of 0.076 mm diam Nb wire, in order to produce the desired magnetic field components *inside* the superconducting shield. The coils allow arbitrary x, y, and z components of magnetic induction to be produced at the trap center with efficiencies of 5–10 μT/mA (in each coil).

To ensure 100%-efficient ''electron shelving'' detection, we need to collect a large fraction of the ions' fluorescence.[7,18] For this reason, the imaging objective lens has a large numerical aperture. Also, it is advantageous to be able to resolve the fluorescence of the individual ions so as to be able to detect them independently using different portions of the photocathode of the imaging UV detector. The lens used in the experiment therefore also has resolving power at 194 nm sufficient to resolve point objects separated by less than 4 μm. The field of view over which the lens can image with aberrations insignificant at this level is about 250 μm. The f number is $f/1$, with the lens's front surface sitting 8.1 mm away from the center of the trap. In order for the lens to be capable of surviving temperature cycles over a range of about 370 K (''bakeout'' temperature during vacuum processing) to 4 K (operational temperature in the experiment), the housing for the five-element lens was constructed of the same UV-grade fused silica as the elements themselves, and the assembly was performed without any bonding agent or cushioning material.

Loading the trap with $^{199}Hg^+$ ions is accomplished by decomposing a sample of isotopically enriched (92%) ^{199}HgO powder in a small ceramic oven tube wound with heater wire, located below the trap. A fraction of the diffuse beam of ^{199}Hg atoms is ionized at the center of the trap by electrons emitted by a field-emitter point. When a sample of ions has been captured, the oven and electron beam are turned off, and the vacuum chamber returns to a uniform 4 K temperature from whatever local warming has occurred.

We first tried loading ions between electrodes L and C [see Fig. 2(a)] and transferring them to the experimental trap. This was unsuccessful. If the ions were loaded between electrodes L and C, we were unable to push them through electrode C into the experimental trap by biasing electrode L

FIG. 5. A linear crystal of laser-cooled $^{199}Hg^+$ ions, illuminated by 194 nm radiation. The gaps are due to the presence of other ions, possibly other mercury isotopes, which do not fluoresce at the same wavelength as $^{199}Hg^+$. The spacing between adjacent ions is $\sim 10\mu$m.

with a positive potential with respect to electrode C (up to about 250 V). This result may have been caused by shielding from the quadrupole rf electrodes and by the non-negligible thickness of the central conical electrode. Subsequent to these experiments, the HgO source and electron source were moved near the experimental trap and the ions were created and captured directly into this trap.

We load and optically resolve individual cold ions, coalesced into linear crystals with interion spacings of 10–30 μm. We have seen crystals ranging in number from one to several tens of ions, very similar in appearance to those reported in Ref. 5. An example is shown in Fig. 5. With laser cooling, these crystals are stable over periods of at least 10 h. One rough measure of the background gas pressure is the rate at which trapped ''impurity'' ions (which show up as readily identifiable nonfluorescing spots in the crystal) exchange places with their $^{199}Hg^+$ ion neighbors. In the room-temperature apparatus at 10^{-8} Pa, these interchanges occurred every few minutes, but they do not occur over periods of several hours or more in our cryogenic vacuum.

We have observed all three ground-state hyperfine microwave transitions ($\Delta M = 0, \pm 1$) by the method discussed in Refs. 5 and 7.

IV. PROSPECTS

We plan to study the microwave transitions in detail after making technical improvements to the magnetic shielding, the nulling of the residual rf micromotion, and the microwave local oscillator frequency synthesis. The scheme for operating this apparatus as a microwave clock will initially be that described for the room-temperature experiment.[5] The ions will be imaged onto separate portions of the detector's photocathode and detected individually as an ensemble of independent atomic clocks. Dehmelt's technique of electron shelving can be used to detect the clock transition in each ion with nearly 100% efficiency.[7,18] Under these assumptions, the fractional frequency stability is given by[8]

$$\sigma_y(\tau) = \frac{1}{\omega_0 \sqrt{N T_R \tau}}, \tag{8}$$

where $\omega_0/2\pi = 40.5$ GHz, N is the number of ions in the linear crystal ensemble, T_R is the free-precession time between the two phase-coherent rf pulses (in Ramsey's interrogation scheme), and $\tau > T_R$ is the averaging time. Assuming a 100 s Ramsey interrogation time, the short-term fractional frequency stability of an ensemble of 30 ions would be $\sim 7\times 10^{-14}\,\tau^{-1/2}$, and longer free-precession times with larger samples of ions seem possible. The fractional second-order Doppler shift to the frequency should be no greater than a few parts in 10^{18} with ions on the trap's nodal center line, cooled to the Doppler limit. The second-order Zeeman shift, as a fraction of 40.5 GHz, is equal to $0.24B^2$, where B is in teslas. Control of this shift may require conventional external magnetic shielding as well as the internal superconducting magnetic shield surrounding the trap. With sufficiently cold ions and small field fluctuations, a fractional inaccuracy of $<1\times 10^{-16}$ of the clock frequency appears attainable.

In addition, this apparatus contains features (the superconducting coil pairs) that should allow us to investigate new effects based on motional Zeeman coherences. These include a novel cooling scheme (proposed by Harde[19]) using optical pumping in conjunction with a motional magnetic coupling between the spin orientation and the harmonic oscillator state of the ions in the trap potential, as well as a scheme for ''squeezing'' the total ensemble spin,[20] which could improve the signal-to-noise ratio in frequency standards where the dominant noise contribution is projection noise.[7]

ACKNOWLEDGMENTS

We thank John Miller for making improvements in the light-collection optics used to acquire the image shown in Fig. 5. We thank Dale Thoele, Doug Gallagher, Richard McLaughlin, and David Kelley for their fine technical support in the construction of the apparatus as well as Donald McDonald and Ronald Ono for their advice on cryogenic matters. We thank John Miller and Joseph Tan for reading the manuscript. This work was supported by the U. S. Office of Naval Research.

[1] F. G. Major and G. Werth, Phys. Rev. Lett. **30**, 1155 (1973).
[2] M. D. McGuire, R. Petsch, and G. Werth, Phys. Rev. A **17**, 1999 (1978).
[3] L. S. Cutler, R. P. Giffard, P. J. Wheeler, and G. M. R. Winkler, in *Proceedings of the 41st Annual Frequency Control Symposium, Philadelphia, 1987* (IEEE, Piscataway, NJ, 1987), pp. 12–19.
[4] R. L. Tjoelker, J. D. Prestage, G. J. Dick, and L. Maleki, in *Proceedings of the 1993 IEEE International Frequency Control Symposium, Salt Lake City, UT, 1993* (IEEE, Piscataway, NJ, 1993), pp. 132–138.
[5] M. G. Raizen, J. M. Gilligan, J. C. Bergquist, W. M. Itano, and D. J. Wineland, Phys. Rev. A **45**, 6493 (1992).
[6] W. M. Itano, L. L. Lewis, and D. J. Wineland, Phys. Rev. A **25**, 1233 (1982).
[7] W. M. Itano, J. C. Bergquist, J. J. Bollinger, J. M. Gilligan, D. J. Heinzen, F. L. Moore, M. G. Raizen, and D. J. Wineland, Phys. Rev. A **47**, 3554 (1993).
[8] D. J. Wineland, J. C. Bergquist, J. J. Bollinger, W. M. Itano, D. J. Heinzen, S. L. Gilbert, C. H. Manney, and M. G. Raizen, IEEE Trans. Ultrason. Ferroelectr. Freq. Control **37**, 515 (1990).
[9] P. T. H. Fisk, M. A. Lawn, and C. Coles, Appl. Phys. B **57**, 287 (1993).
[10] J. D. Prestage, G. J. Dick, and L. Maleki, J. Appl. Phys. **66**, 1013 (1989).
[11] H. G. Dehmelt, in *Frequency Standards and Metrology, Proceedings of the 4th Symposium, Ancona, Italy, 1988,* edited by A. DeMarchi (Springer-Verlag, Berlin, 1989), p. 286.
[12] W. Paul, O. Osberghaus, and E. Fischer, Forschungsber. Wirtsch. Nordrhein-Westfalen, Nr. 415 (1958).
[13] W. M. Itano and D. J. Wineland, Phys. Rev. A **25**, 35 (1982).
[14] D. J. Wineland, J. C. Bergquist, J. J. Bollinger, W. M. Itano, F. L. Moore, J. M. Gilligan, M. G. Raizen, D. J. Heinzen, C. S. Weimer, and C. H. Manney, in *Laser Manipulation of Atoms and Ions, Proceedings of the International School of Physics "Enrico Fermi," Course CXVIII, Varenna,*

Italy, edited by E. Arimondo, W. D. Phillips, and F. Strumia (North-Holland, Amsterdam, 1992), pp. 553–567.
[15] G. Gabrielse, X. Fei, W. Jhe, L. A. Orozco, J. Tan, R. L. Tjoelker, J. Haas, H. Kalinowsky, T. A. Trainor, and W. Kells, Am. Inst. Phys. Conf. Ser. **233**, 549 (1991).
[16] C. C. Lim, Rev. Sci. Instrum. **57**, 108 (1986).
[17] W. W. Macalpine and R. O. Schildknecht, Proc. IRE **47**, 2099 (1959).
[18] H. G. Dehmelt, IEEE Trans. Instrum. Meas. **IM-31**, 83 (1982).
[19] H. Harde, in *International Conference on Quantum Electronics Technical Digest, Series 1990* (Optical Society of America, Washington, DC, 1990), Vol. 8, p. 278.
[20] D. J. Wineland, J. J. Bollinger, W. M. Itano, F. L. Moore, and D. J. Heinzen, Phys. Rev. A **46**, R6797 (1992); D. J. Wineland, J. J. Bollinger, W. M. Itano, and D. J. Heinzen, *ibid.* **50**, 67 (1994).